Front. Environ. Sci. Eng. 2021, 15(6): 113
https://doi.org/10.1007/s11783-021-1401-y

RESEARCH ARTICLE

Effective remediation of organic-metal co-contaminated soil by enhanced electrokinetic-bioremediation process

Fu Chen (✉)[1,2], Qi Zhang[2,3], Jing Ma[1], Qianlin Zhu[1], Yifei Wang[2,3], Huagen Liang[1]

1 Low Carbon Energy Institute, China University of Mining and Technology, Xuzhou 221008, China
2 School of Environmental Science and Spatial Informatics, China University of Mining and Technology, Xuzhou 221008, China
3 School of Public Policy and Management, China University of Mining and Technology, Xuzhou 221116, China

HIGHLIGHTS

- A new EK-BIO technology was developed to decontaminate e-waste contaminated soil.
- Adding sodium citrate in electrolyte was a good choice for decontaminating the soil.
- The system has good performance with low cost.

GRAPHIC ABSTRACT

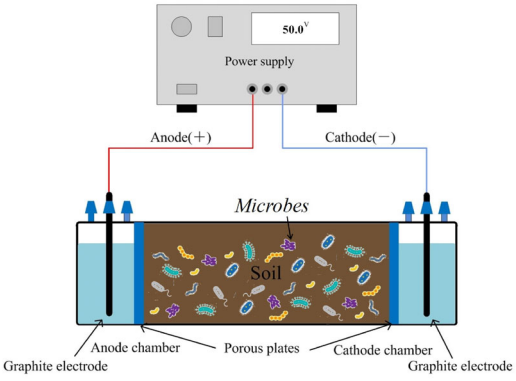

ARTICLE INFO

Article history:
Received 20 October 2020
Revised 15 November 2020
Accepted 6 December 2020
Available online 4 February 2021

Keywords:
Electrokinetic
Co-contamination
Debromination

ABSTRACT

This work investigates the influence of electrokinetic-bioremediation (EK-BIO) on remediating soil polluted by persistent organic pollutants (POPs) and heavy metals (mainly Cu, Pb and Ni), originated from electronic waste recycling activity. The results demonstrate that most of POPs and metals were removed from the soil. More than 60% of metals and 90% of POPs in the soil were removed after a 30-day EK-BIO remediation assisted by citrate. A citrate sodium concentration of 0.02 g/L was deemed to be suitable because higher citrate did not significantly improve treatment performance whereas increasing dosage consumption. Citrate increased soil electrical current and electroosmotic flow. After remediation, metal residues mainly existed in stable and low-toxic states, which could effectively lower the potential hazard of toxic metals to the surrounding environment and organisms. EK-BIO treatment influenced soil microbial counts, dehydrogenase activity and community structure.

1 Introduction

Organic-metal co-contamination has become an important environmental concern in the world (Lu et al., 2014; Han et al., 2018; Li et al., 2018; Tang et al., 2020). There exist quite different chemical processes and remediation mechanisms between organic and metal pollutants. Thus remedying organic-metal combined pollution is more complex than individual pollution.

Complicated interactions can occur between organic and metal contaminants in soil. There may be competition between organic and metal pollutants for adsorption sites on soil, which will inevitably lead to the mutual restriction of their adsorption process. For example, the adsorption of chromate and arsenate on soil surface was often disturbed by coexisting anions (such as plant rhizosphere exudates), but the presence of cations has little effect on them (Pradas del Real et al., 2014). The adsorption behavior of organic acids on mineral surface could be influenced by metal ions, and the effect was enhanced with the increase of ion charge number (Uddin, 2017). The coexistence of organic

✉ Corresponding author
E-mail: chenfu@cumt.edu.cn

pollutants and heavy metals can form organometallic complexes, which will significantly change the physic-chemical behavior of organic and metal pollutants in the soil. For example, mercury, tin and other metals can interact with organic pollutants to form more toxic organometallic compounds (such as methylmercury, trimethyltin and so on) (Li et al., 2012). Thus, the remediation of organic-metal co-contamination involves complicated mechanisms, and the task is far more difficult than that of single contamination. Therefore, it is critical to study and develop eco-friendly and efficient processes to remediate organic-metal co-contamination.

As a green remediation technology developed recently, the electrokinetic (EK) process has exhibited advantages such as simplicity and safety (Virkutyte et al., 2002). Moreover, EK technology can be used to treat soils with fine texture and low-permeability, which are difficultly accessible for other treatment techniques (Virkutyte et al., 2002). Nevertheless, organic and metal pollutants cannot be removed simultaneously by conventional EK approaches due to the heavy metal accumulation and the weak migration of organic contaminants (Gomes et al., 2012).

Recently, a new technology, the electrokinetic-bioremediation (EK-BIO) technique has been developed for remedying organic-polluted soil and groundwater. It can enhance the mass transfer between organic pollutants and degrading bacteria in the soil, and may transport various additives (active microbes, nutrients and electron acceptors, etc.) to the polluted area to improve the efficiency of bioremediation through various electrokinetic effects (such as electroosmosis, electromigration and electrophoresis) (Hassan et al., 2016; Wang et al., 2016; Ramadan et al., 2018). In recently years, because of its advantages including high efficiency, no secondary pollution and energy saving, EK-BIO has been widely concerned by soil remediation experts (Hassan et al., 2016; Wang et al., 2016; Ramadan et al., 2018).

At present, EK-BIO was mainly employed to remediate organic-contaminated soil, but it was seldom used in the treatment of organic-metal co-contamination. In the present work, EK remediation and bioremediation were combined to synchronously extract heavy metals and oxidize organic pollutants from electronic waste (e-waste) recycling polluted soil. This investigation aim was to find a rapid, economical, efficient, and secure technology to decontaminate soil contaminated by e-waste recycling activity.

2 Materials and methods

2.1 Reagents

Deuterated and ^{13}C labeled POPs standards were purchased from Wellington Laboratories (Ontario, Canada). Other chemicals were purchased commercially.

2.2 Contaminated soil

The contaminated soil studied in this work was collected from Xuzhou, Jiangsu Province, China. The soil was characterized by: pH 6.7, total organic carbon (TOC) 2.56 wt.%, polyaromatic hydrocarbons (PAHs) 380 mg/kg, polychlorinated biphenyls (PCBs) 175 mg/kg, polybrominated diphenylethers (PBDEs) 124 mg/kg, Cu 860 mg/kg, Pb 655 mg/kg, Ni 588 mg/kg. The details of pollutants were given in Tables S1–3, Supporting Information.

2.3 The design of experiments

The EK-BIO experimental system used in this work was the same as that described in previous work (Ma et al., 2020). The soil chamber had a dimension of 25 cm × 12 cm × 12 cm loaded with 2 kg of dry soil. A filter paper (pore size 30−50 μm) was placed between the soil and the porous stone in front of the electrodes to preclude the penetration of soil particles into the electrolyte reservoirs. The voltage gradient was maintained at 2.0 V/cm by using a direct-current power supply. $NaNO_3$ solution (0.01 g/L) was employed as the supporting electrolyte (Ma et al., 2020). To control possible anode acidification and cathode alkalization, the pH of electrolyte was controlled at the soil background pH (6.7) with an automatic pH controller.

An aqueous solution containing inorganic salts was added to the soil to provide 20% (w/w) water content. The medium composition was as follows (g/L): $NaNO_3$ 1.5, $(NH_4)_2SO_4$ 1.5, K_2HPO_4 1.0, KCl 0.5, $MgSO_4 \cdot 7H_2O$ 0.5, $FeSO_4 \cdot 7H_2O$ 0.01, $CaCl_2$ 0.002. The medium pH was 7.0.

Table 1 summarizes the test conditions. The electrolyte solution was renewed every three days to keep consistent properties. The tests were carried out at 25±2°C, and all

Table 1 Summary of the experimental conditions employed in this work

Test	Anolyte solution	Catholyte solution	Voltage gradient (V/cm)
T0	0.01 g/L $NaNO_3$	0.01 g/L $NaNO_3$	–
T1	0.01 g/L $NaNO_3$	0.01 g/L $NaNO_3$	2.0
T2	0.02 g/L citrate sodium−0.01 g/L $NaNO_3$	0.02 g/L citrate sodium−0.01 g/L$NaNO_3$	2.0
T3	0.05 g/L citrate sodium−0.01 g/L $NaNO_3$	0.05 M citrate sodium−0.01 g/L $NaNO_3$	2.0

aqueous solutions were prepared using high-purity water. Soil water content was maintained at about 20% by regular supplement of sterile inorganic medium. At regular intervals, the soil was removed from the apparatus, cut into five equal slices (S1–S5, from anode to cathode) and analyzed for various physical-chemical and microbial parameters.

2.4 Analysis methods

Electrical current (EC) was determined with an EC meter (model DDS-11A, Shanghai REX Instrument Co., Ltd., China). Soil pH was determined by using a pH meter (model pHS-3B, Shanghai Precision Scientific Instrument Co., Ltd., China). TOC was determined using a TOC analyzer (Shimadzu TOC-VCPH, Kyoto, Japan) through catalytic oxidation. Zeta potential was measured using a zeta potential analyzer (Malvern, Zetasizer Nano, ZS90, UK). Electroconductivity was measured using an analyzer (model DDS-307A, Shanghai Leici Co., Ltd, China). Bromide ions were determined by ion chromatography (C196-E039 A, Shimadzu, Japan) with a Shim-pack IC-A3 chromatographic column. Total bromine was determined by inductively coupled plasma optical emission spectrometry (ICP-OES, model Optima 4100 DV, Perkin Elmer, USA) after pretreatment using oxygen bomb combustion.

2.5 POPs and metals analysis

The details of the extraction and analysis of persistent organic pollutants (POPs) and heavy metals are given in the Supporting Information. Metals were fractionized into five different fractions namely water soluble and exchangeable fraction (F1), carbonates-bound fraction (F2), Fe-Mn oxides-bound fraction (F3), organic matter-bound fraction (F4), and residual fraction (F5) (Mahanta and Bhattacharyya, 2011).

2.6 Microbial analysis

Total heterotrophic bacteria (THB) were counted by the dilution plating method on nutrient agar. After 2 days of incubation at 28°C, bacterial colonies in the plates were counted and the results were expressed as colony forming units (CFU) per gram of dry soil.

Microbial dehydrogenase activity (DHA) was determined according to Lu et al. (2009), and the results were expressed as μg triphenyl tetrazolium formazan (TPF) per gram of soil.

2.7 PLFA analysis

Analysis of total phospholipid fatty acids (PLFAs) was conducted following the description of Li et al. (2020). Gram-positive/gram-negative bacteria (GP/GN) ratio and stress indicator (cy/pre) were used to evaluate the variations of bacterial community structure in soil and potential bacterial stress, respectively.

3 Results and discussion

3.1 Variation in electroosmotic flow

According to the electric double layer theory (Pletcher et al., 2010), the initial soil had a negative zeta potential (−1.26 mV), thus the direction of electroosmotic flow (EOF) was from the anode to the cathode. When EC is fixed at a certain level, the relationship between zeta potential (Z) and soil solution pH is as follows (Lorenz, 1969):

$$Z(\mathrm{mV}) = -38.6 + 281e^{-0.48\mathrm{pH}}. \quad (1)$$

The surface charge of soil is zero at pH 4. During EK treatment, the acid produced at the anode moves faster than the anion produced at the cathode, and the acid formed at the cation moves toward the cathode, resulting in the variation of zero charge potential on the soil surface. On the basis of the Helmholtz-Smoluchowski theory, increasing soil zeta potential can inhibit the rate of EOF, and even alter the direction of EOF (Sharma and Reddy, 2004).

In this work, the zeta potential of soil samples from various tests was constantly negative and thus no reverse direction of EOF occurred. Figure 1A shows the accumulative EOF under different conditions. EOF could deliver nutrients, citrate and its derivatives through the soil column for interacting with microbes and heavy metals. T3 had the highest EOF (883 mL), followed by T2 (720 mL) and T1 (512 mL), whereas no EOF was detected in T0 (Fig. 1A). No electric current was applied in T0, thus no EOF in this test was understandable. The addition of citrate (T2 and T3) could increase ionic strength of solution and soil, thus promote EOF. As a chelating regent, citrate could improve the generation of negatively charged complexes; soil zeta potential became more negative, leading to enhanced mobility of electrolytes (Weng and Yuan, 2001). Soil zeta potential values were −26, −63 and −105 mV for T1, T2 and T3, respectively, which declined with increasing citrate concentration, suggesting the chelation of citrate with metals. Thereupon, higher EOF values were observed in T2 and T3 relative to T1 (Fig. 1A). These results indicate that adding citrate could modify the interactions among solution, zeta potential and soil particles, thus affecting EOF.

3.2 Electrical current change

Figure 1B shows the changes of electrical current (EC) with time during the tests. The soil had a starting EC value of 11.4 mA. The EC of each experimental group decreased slightly in the first day, and then gradually increased. In the course of EK, EC can be affected by the conductivity of

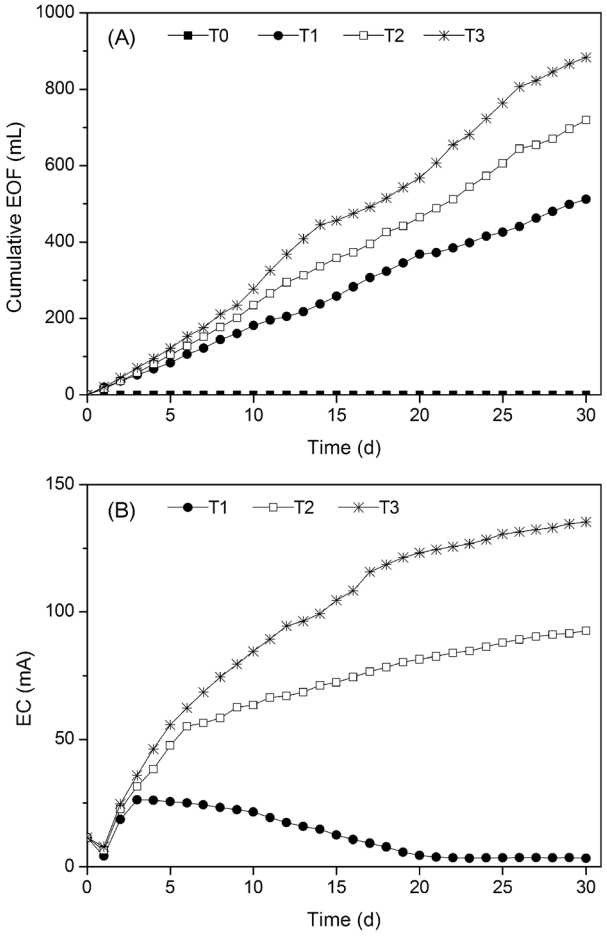

Fig. 1 Change of cumulative EOF (A) and EC (B) with time during treatments.

soil pore water, electrolyte composition and soil humidity. The ion concentration in pore water decreased with time, and Ca^{2+}, Mg^{2+} and Al^{3+} ions in the soil may form hydroxide precipitates with OH^- produced in the cathode, leading to decreased conductivity and EC. Nevertheless, with the continuous supplement of electrolyte into the soil, the number of Na^+ ions in the soil increased significantly, thus the EC increased in this stage. Moreover, clay flocculation may occur due to the decrease of EOF and pH value near the anode. This would cause a more open soil structure, and thus promote the dissolution of residual salt and increase the current (Virkutyte et al., 2002; Hassan et al., 2016).

In T1, the EC value was maximized (26.3 mA) on day 3, and then it declined to about 3.5 mA and kept stable until the end of tests (Fig. 1B). In T2 and T3, EC continuously increased, and a maximum value of 92.6 and 135.3 mA was obtained for T2 and T3, respectively, at day 30. Heavy metals can be released from soil by citrate through ion exchange and electrostatic attractions (Suanon et al., 2016). Thereupon, the concentration of heavy metal ions in pore water may increase after the introduction of citrate into soil from the anode chamber. The EC value would increase with increasing the content of mobile ions (Acar and Alshawabkeh, 1993).

3.3 Soil pH and electroconductibility

Figure 2 exhibits the change in soil pH and electroconductibility across soil sections after 30 days of tests. In T0, various parameters varied little. In T1, T2 and T3, the pH increased from 6.3 to 6.5 (S1) to around 6.9−7.2 (S5) (Fig. 2A). Adding citrate reduced soil pH relative to T1, and the pH values in T2 and T3 was less than that in T1.

In this work, the control of electrolyte pH brought stable soil pH, which was beneficial for the bioremediation of organic pollutants, since near-neutral pH conditions are most favorable for biodegradation. In general, in the process of EK remediation, H^+ ions produced in the anode chamber moved toward the cathode faster than OH^- ions toward the anode, resulting in the lowering of soil pH in sections near the anode. Usually EK reactions would cause significant changes in soil pH, namely acidification in the near-anode region and alkalization in the near-cathode

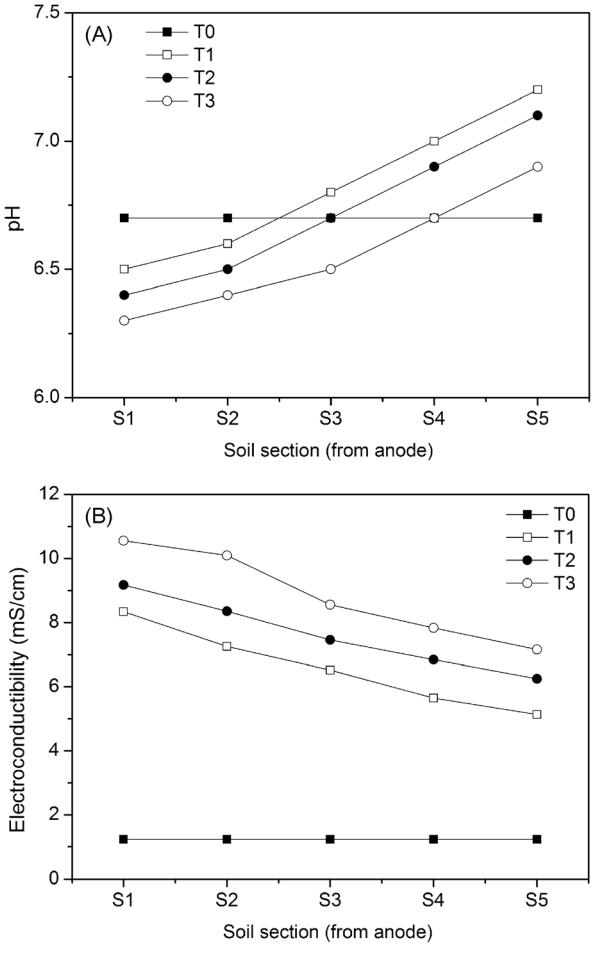

Fig. 2 Changes of (A) pH and (B) electroconductibility in soil sections after 30 days of treatments.

region, because of the massive production of protons and hydroxyl ions at the anode and cathode, respectively (Acar and Alshawabkeh, 1993). With the continuous decrease of pH, the net surface charge and zeta potential of soil would become positive. According to the theory of electric double layer, EOF moving toward the cathode would gradually weaken, and finally the direction of EOF can be reversed (Sharma and Reddy, 2004). The desorption of heavy metals from soil particles and the direction of EOF are affected by soil pH. Thus substantial change in soil pH would restrict the efficiency of EK remediation.

The variation of soil electroconductibility before and after 30 days of tests is shown in Fig. 2B. The distribution of electroconductibility obeyed a similar pattern as soil pH. At higher pH conditions, metal ions may precipitate and thus reduce the number of mobile ions and thus lower soil electroconductibility. Additionally, T3 exhibited significantly higher electroconductibility value than other groups. This is because that the introduction of citrate increased the electroconductibility of electrolyte; meanwhile, citrate could chelate with heavy metals and thus increase ion concentration in the soil, resulting in the increase of electroconductibility.

3.4 Distribution and removal of toxic metals

Heavy metals are one group of main pollutants in e-waste polluted soil, and the biodegradation activity of POPs can be inhibited by the presence of high levels of heavy metals. Thus, the removal efficiency of toxic metals is vital for POPs remediation in the soil (Lu et al., 2014). To study the shift of heavy metals within the soil column, the measured concentrations of individual metals in different soil sections were normalized to their initial concentrations.

In T0, no detectable change was observed for the level of soil metals, thus the related data were not demonstrated. During the tests, heavy metals were detected in both anolyte and catholyte (Table 2). Under the action of an electric field, the complex anions of $[M(II)\text{-citric}]^-$ in soil migrated to the anolyte; while those non-chelated metals migrated to the catholyte. In T1, a small amount of heavy metals detected in the anolyte was ascribed to the dissolution of soil metals from the adjacent sections. The introduction of citrate significantly increased the cumulative amount of metals (especially Pb) in the electrolyte (Table 2).

In T1, large amounts of metals moved from anodic sections and cumulated near the cathode; the C/C_0 value was 0.52, 0.68, 0.82, 1.25 and 1.36 for sections 1–5, respectively; the Pb content (C/C_0) was 0.63, 0.77, 0.91, 1.37 and 1.45 for sections 1–5, respectively; the Ni content (C/C_0) was 0.34, 0.45, 0.66, 0.82 and 1.05 for sections 1–5, respectively (Fig. 3A). Typically, Cu, Pb and Ni existed in their divalence oxidation state; thus they were expected to move to cathode. Nevertheless, Cu^{2+}, Pb^{2+} and Ni^{2+} ions begin to precipitate at pH values of 4.5, 4.5 and 5.9, respectively (Salzberg, 1983). Thus the desorption efficiency of the three metals was not high in T1. The closer to the cathode, the higher the metal content (Fig. 3A), indicating the precipitation of a considerable amount of metals in Sections 4 and 5. Thus, metal removal was low.

T2 exhibited significantly higher metal elimination than T1 (Table 3), indicating that adding citrate benefited metal electro-migration by continuous provision of mobile ions in soil. The anionic citrate in the cathode compartment was expected to migrate toward the anode under the action of electric field. In this process, negatively-charged citrate ions would continuously complex metal ions in the soil to form $[M(II)\text{-citric}]^-$ ions which electromigrated toward the anode. The contribution of EOF to metal elimination is low under soil conditions, whereas electro-migration becomes the predominant transportation mechanism for the charged metal chelates (Dong et al., 2013). The results of the present work supported this view, namely most metals accumulated in the anolyte (Table 2, T2). When citrate sodium was applied (T2), metal contents decreased gradually from S5 to S1 with small differences (Fig. 3B), and all C/C0 values were below 1, demonstrating effective removal of metals from the soil. In general, S5 had the lowest metal content among five soil sections (Fig. 3B). The soil sections close to the cathode came into contact with the greatest quantity of citrate and superior soil–solution–pollutant interactions, resulting in greater degree of desorption and migration of metal ions across the soil column. Finally, high removal of metals (74.5% Cu, 63.6% Pb, and 82.3% Ni) was obtained, which was significantly higher than that of T1 (Table 2). The results show that under the same conditions, the removal efficiency of metals followed the order Ni>Cu>Pb, which is consistent with other reports (Naghipour et al., 2016; Song et al., 2016).

When citrate sodium concentration was increased from

Table 2 Metal mass distribution in the soil and electrolyte after 30 days of treatment

Distribution (%)	T1			T2			T3		
	Cu	Pb	Ni	Cu	Pb	Ni	Cu	Pb	Ni
Anolyte	0.3	0.3	4.5	69.2	60.2	60.7	79.7	68.2	74.2
Soil	92.6	95.8	67.4	25.5	36.4	17.7	15.5	28.7	9.4
Catholyte	7.1	3.9	28.1	5.3	3.4	21.6	4.8	3.1	16.4
Total removal	7.4	4.2	32.6	74.5	63.6	82.3	84.5	71.3	90.6

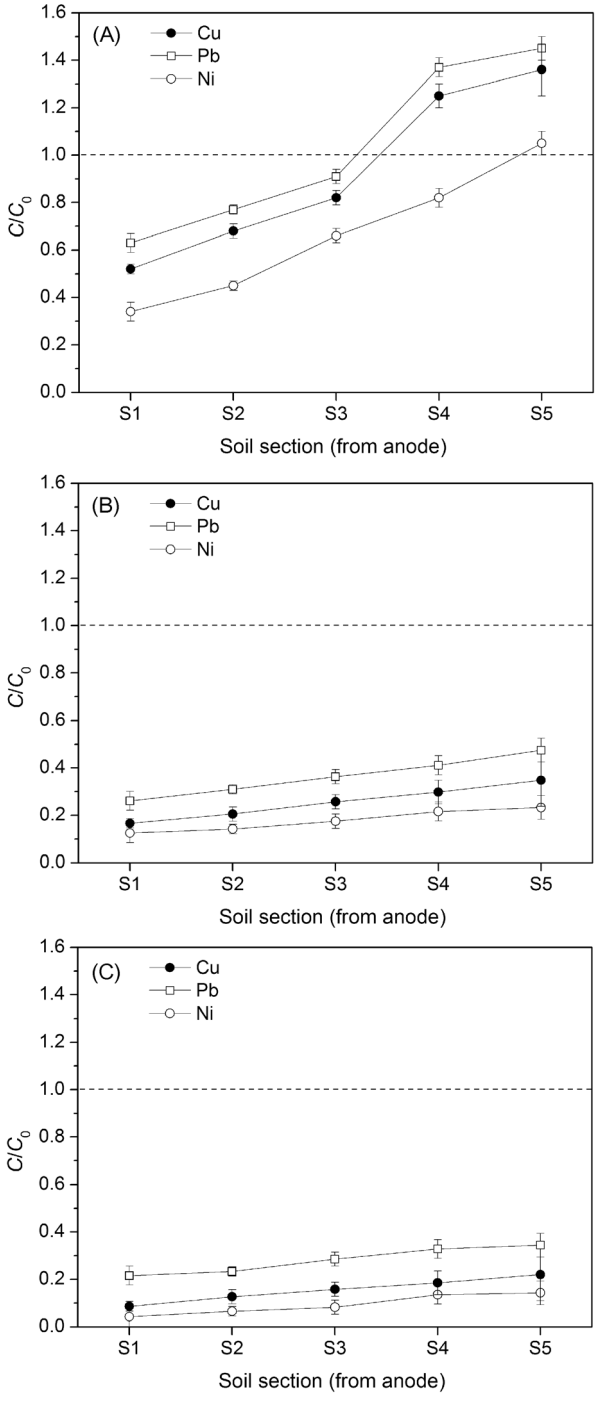

Fig. 3 Ultimate contents (C/C_0) of metals in the soil of T1 (A), T2 (B) and T3 (C) after 30 days of treatment (the initial metal contents in each soil section were represented by the horizontal lines).

0.02 to 0.05 M, the mobility and removal of various metals were further enhanced (Fig. 3C), yielding 84.5% of Cu, 71.3% of Pb and 90.6% of Ni removals (Table 2). Apparently, increasing citrate dosage could improve metal mobility and migration. Nevertheless, 2.5 times increase of citrate dosage only brought about an improvement of metal removal by less than 10 percentage points (Table 2).

3.5 Metal fractionation changes

Extraction with citrate caused the significant reduction of F1, F2 and F3 fractions of Cu, Pb and Ni, whereas F4 and F5 fractions were rarely touched (Table 3). In general, exchangeable/acid soluble fraction (F1 and F2) and reducible fraction (F3) are the major groups that can be influenced by chelating agents. In this work, most of the extracted Cu or Ni by citrate was from F1 and F2 fractions, while most of the extracted Pb was from F3 fraction. The significant reduction of F1 and F2 fractions for soil Pb was also found. F1, F2 and F3 fractions contributed greatly to the quantity of citrate extracted Cu. On the basis of the sequential extraction procedure, metals liberated in steps 1 and 2 were comprised of exchangeable ions (F1) and carbonates (F2), respectively, while reducible fraction (F3) consisted of hydroxides or oxides associated with Fe/Mn oxides (Cappuyns et al., 2007). Exchangeable ions may also be desorbed by chelating agents. Chelating agents can greatly increase the solubility of carbonates. Therefore, F1 and F2 fractions are more easily extracted by citrate. The reaction of metal oxides with chelating agents could lead to the release of the related metals (Nowack, 2002). Compared to F1, F2 and F3 fractions, it is difficult for F4 (related to sulfides and organic substances) and F5 (combined in crystal matrix) to release in the presence of chelating agents.

3.6 POPs elimination by simultaneous extraction and oxidation

POPs were not detected in anolyte, and 4.8%–6.3% of POPs were transported into catholyte by EOF (Table 4). Apparently, higher EOF could produce greater POPs movement. In T0, it was found that POPs were evenly distributed throughout the soil sections (Fig. 4). EK application improved POPs elimination in soil relative to T0. In T1, there was a pattern of slight increase in the C/C_0 value of POPs from anode to cathode, whereas no ordered distribution of POPs residue was observed in T2 and T3 (Fig. 4). In T1, T2 and T3, the POPs content (C/C_0) of S1-S5 was in the range of 0.32–0.40, 0.056–0.123 and 0.063–0.085 (Fig. 4), respectively, leading to POPs removal efficiency of 63.4%, 91.6% and 92.8%, respectively (Table 4). Apparently, EK could promote biodegradation of POPs in the soil. Moreover, citrate application significantly increased POPs removal compared to T1, but the difference between T1 and T2 was little.

In general, the presence of high levels of toxic metals could inhibit biodegradation of organic pollutants in soil (Dong et al., 2013). The effective removal of metals in T1 may enhance biodegradation of POPs through reducing soil metal contents (Fig. 4). EK operation, especially

Table 3 The fractionation changes of metals (mg/kg) at soil section S1 of group T2 after 30 days of treatment

Metal	Untreated					Treated				
	F1	F2	F3	F4	F5	F1	F2	F3	F4	F5
Cu	494.9	185.8	104.5	51.6	23.2	21.2	12.4	39.6	48.3	21.5
Pb	383.4	131.4	95.2	24.7	20.3	51.8	41.8	36.3	22.5	18.6
Ni	296.4	145.2	116.3	18.5	11.6	11.5	19.1	23.2	12.4	7.8

Note: F1, water soluble and exchangeable fraction; F2, carbonates-bound fraction; F3, Fe-Mn oxides-bound fraction; F4, organic matter-bound fraction; F5, residual fraction.

Table 4 POPs mass distribution in the soil and electrolyte after 30 days of treatment

Distribution (%)	T0	T1	T2	T3
Anolyte	ND	ND	ND	ND
Soil	76.7	36.6	8.4	7.2
Catholyte	ND	4.8	5.9	6.3
Total removal	23.3	63.4	91.6	92.8

ND: not detected.

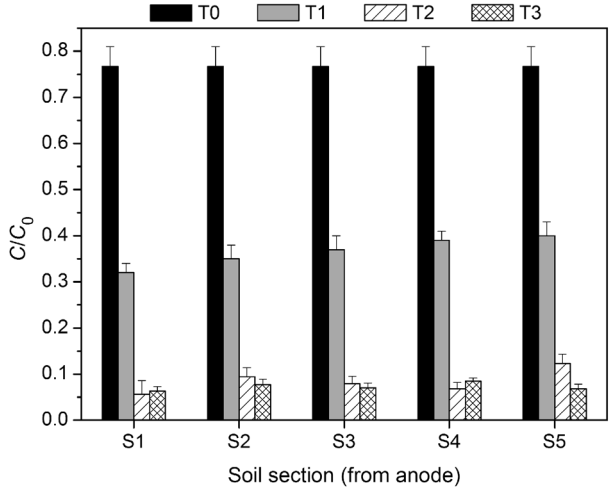

Fig. 4 Ultimate contents (C/C_0) of POPs in the soil after 30 days of treatment.

complexation of metals by chelating agent, may reduce the level of soil metal ions and therefore lighten the inhibitory influence on the microflora. Additionally, EK treatment can lead to a more homogeneous distribution of nutrients, promoting microbial migration and pollutant bioavailability in soil. The results of POPs removal reflected the collaborative impacts of bioremediation and EK processes for achieving the improved removal of POPs. Due to their high hydrophobicity, POPs (PBDEs, PAHs and PCBs) in this work were less removed by EOF (Table 4). During EK-BIO treatment, organic pollutants can be degraded by both microbes and electrochemical mechanisms such as Cl_2, ClO^- and H_2O_2, which are produced by anodic reaction and water electrolysis reaction (Zhang et al., 2017). To identify potential abiotic degradation of POPs during EK-BIO treatment, an abiotic control (Autoclaved soil was supplemented with 0.5% NaN_3, 50 V voltage) was set up and operated along with normal tests. Results demonstrate that abiotic loss of POPs (not including accumulation in electrolyte) was about 17.6% of initial content of POPs in the soil (Table S4 in the Supporting Information). Therefore, the enhanced removal of POPs in EK-BIO trials (T1, T2 and T3) was mainly due to the improvement of biodegradation (Table 4).

3.7 Debromination of PBDEs

Br and Cl are the constituents in the gecules of PBDEs and PCBs, respectively; thereupon, monitoring the concentrations of released Br and Cl can indicate the decomposition of PBDEs and PCBs, respectively. The soil and nutrient solution contained a large amount of chloride ions; therefore chlorine ions were not measured. The dissociation of C–Br bond in PBDEs was further verified by observing the transformation of Br atoms. No high valence bromine ions were detected in this work. To investigate the fate of PBDEs, the content of Br^- ions in soil and electrolyte was determined and normalized by the total amount of bromine.

As shown in Fig. 5, T2 and T3 showed greater soil Br^- content than T0 and T1, which was in agreement with the results of POPs elimination (Table 4). As far as electrolyte is concerned, no Br_2 was detected in both anolyte and catholyte, wherein Br^- ions appeared (Fig. 5). The content of Br^- ions in soil was low (less than 14%), and a small amount of Br^- ions (1.4%–2.1%) was detected in catholyte, whereas Br^- ions converged in anolyte (23.4%–46.3%). Br^- ions could move to anode by electromigration due to its negative charge. In this work, no Br_2 was detected, indicating no Br^- oxidation by anodic reactions occurred, though which was reported previously (Chen et al., 2019). The debromination ratio of PBDEs was 8.6%, 36.4%, 58.6% and 62.2% in T0, T1, T2 and T3, respectively, which was lower than the corresponding PBDEs degradation (22.9%, 63.1%, 90.4% and 92.0%, respectively). This result suggests the formation and accumulation of a few Br-containing organic intermediates.

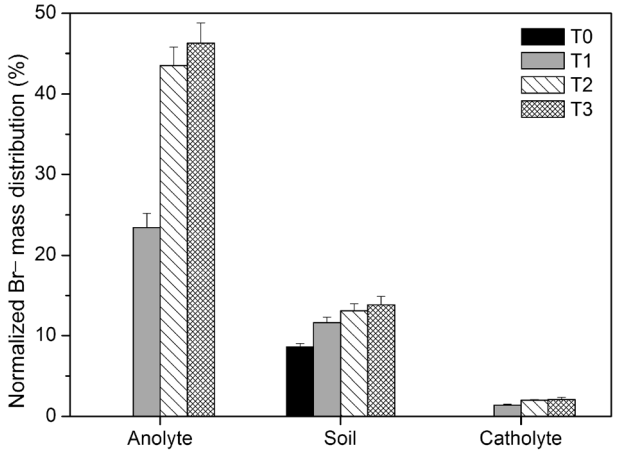

Fig. 5 The normalized mass distributions of Br^- ions in soil and electrolyte after 30 days of EK-BIO treatment. The data were obtained by normalizing the release amount of Br^- ions to the total bromide content of PBDEs in the untreated soil.

3.8 Microbial enumeration and dehydrogenase activity

Figure 6A demonstrates the variation of THB density in soil before and after EK-BIO remediation. The initial THB density was about 4.58×10^6 CFU/g soil. After 30 days, THB density was apparently higher in EK-BIO applied soils (T1, T2 and T3) compared with T0 (Fig. 6A). Soil THB count followed the order of T3>T2>T1>T0>initial, which accorded with the result of POPs elimination. Moreover, THB number increased from anode to cathode for some tests, indicating the occurrence of bacterial movement in the soil due to the application of weak electric field. These results suggest that the growth and reproduction of soil bacteria may be enhanced through electric field application. Many factors (such as electrophoresis, electroosmosis and nutrient flow) can influence the transport and distribution of soil microorganisms under electric field (Dong et al., 2013). Therefore, the final distribution of soil bacteria under electric field depends on the competitions among electrophoresis, electroosmosis and nutrient flow.

Figure 6B shows soil DHA change in various soil sections before and after remediation. In general, the DHA values were in the order: T3>T2>T1>T0>initial. DHA was highest in S5 of T3 (74.6 μg TPF/g soil), which was 2.7 times that of initial level (27.5 μg TPF/g soil). It can be found that the change of bacterial density was basically in agreement with that of DHA. The formation of oxygen in anode can increase the content of dissolved oxygen in soil, and improve the respiration of microorganisms and indirectly enhance the redox level of soil, therefore promoting DHA and favoring POPs biodegradation.

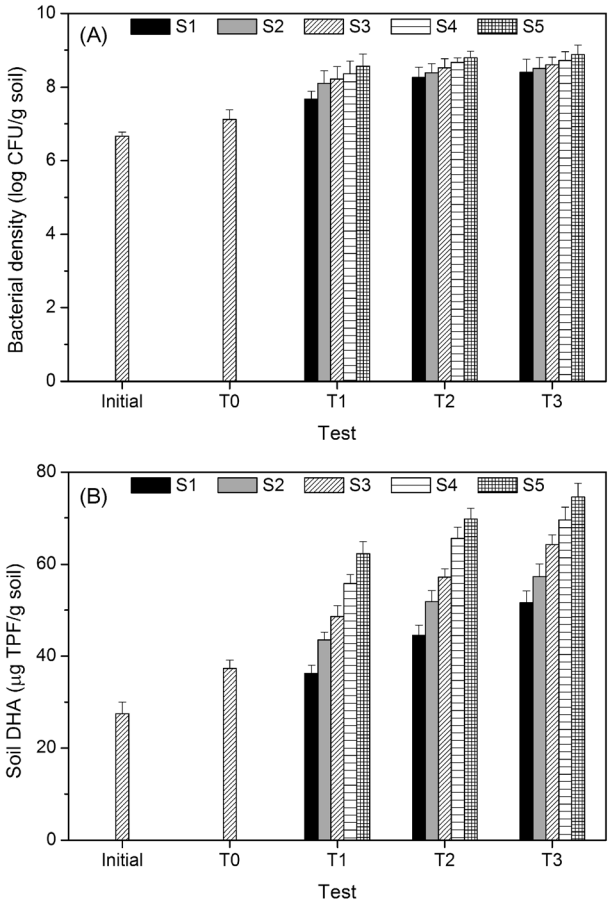

Fig. 6 Soil bacterial density (A) and DHA (B) before and after 30 days of remediation across various soil sections (S1–S5). For simplicity, only one value was demonstrated for initial and T0 since no difference among various soil sections was negligible.

3.9 Evolution of microbial community structure and diversity

Figure 7A shows the influence of EK-BIO treatment on the spatial changes of GP/GN ratio. It can be found that the GP/GN ratio went up in the treated soils relative to the initial one. The GP/GN ratio showed a decreasing trend from anode to cathode in T1, but no ordered arrangement of GP/GN ratio among soil sections of one test in T2 and T3 (Fig. 7A). Basically, the GP/GN ratio followed the order of T3>T2>T1>T0>initial. There existed a positive relation between the GP/GN ratio and POPs removal extent, namely negative relationship between the GP/GN ratio and the residue ratio (C/C_0) of POPs (Fig. 4). GP/GN is indicative of the relative dominance of Gram-positive and Gram-negative bacteria, and the increment in GN PLFAs could be correlated with stress conditions (Li et al., 2020).

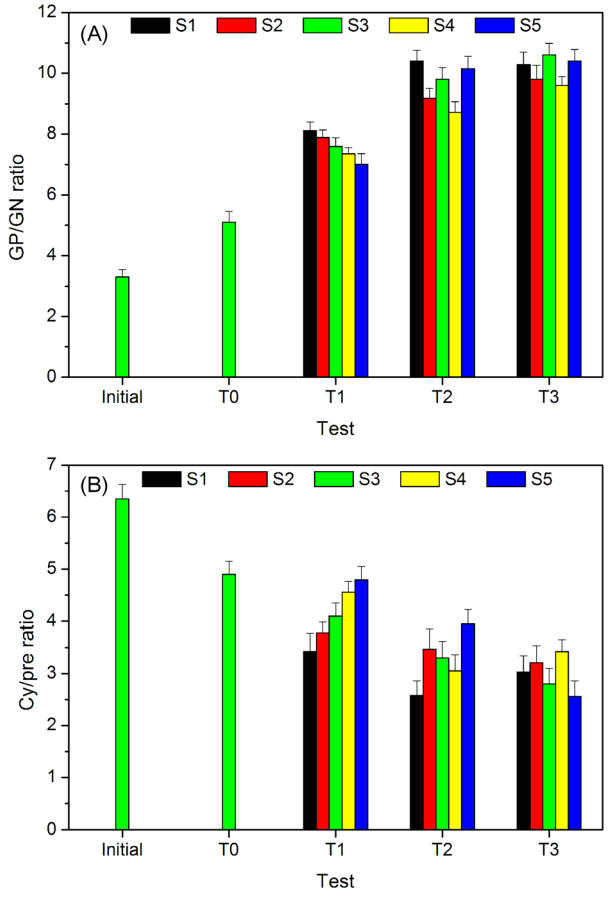

Fig. 7 Changes of GP/GN (A) and cy/pre (B) ratios in the tests before and after 30 days of remediation across various soil sections (S1–S5). For simplicity, only one value was demonstrated for initial and T0 since no difference among various soil sections was negligible.

Figure 7B demonstrates cy/pre ratio before and after treatment. Compared with initial soil, the cy/pre ratio reduced after treatment. The cy/pre ratio declined in the order initial>T0>T1>T2>T3. By comparison, it can be found that the variation trend of cy/pre value was contrary to the change of POPs removal extent and the GP/GN ratio (Fig. 4). Cy/pre is associated with the growth rate of bacteria rate and soil carbon levels (Yao et al., 2016). High cy/pre values indicate the inhibited proliferation of bacteria and the predominance of stationary growth phase (Kakosová et al., 2017).

The correlation coefficients between removal extent of POPs and bacterial PLFAs were 0.473, 0.885, 0.926 and 0.905 ($P < 0.05$, data not shown) for T0, T1, T2 and T3, respectively, indicating that the bacteria played an important role in POPs degradation. This result supports the findings of Li et al. (2020), which demonstrated a positive relationship between the GP/GN ratio and the degradation degree of PAHs, whereas a negative relationship was observed between the cy/pre value and the removal degree of PAHs during EK-BIO treatment.

4 Conclusions

In this work, a EK-BIO system was used to remedy e-waste contaminated soil by addition of chelating agent. Results show that adding sodium citrate in electrolyte was a good choice to remediate the metal–organic co-contaminated soil. Citrate addition enhanced the formation of [M(II)-citric]$^-$ complexes that could generate higher EC and electroconductibility. The results also demonstrate that remediation treatment affected microbial activity and community structure. A citrate sodium concentration of 0.02 g/L was appropriate for the completion of remediation practice. On the basis of the overall results of this work, it can be concluded that the EK-BIO process by stimulating indigenous bacteria with the addition of citrate can be a good treatment approach to remediate metal-organic co-contaminated soil.

Acknowledgements This work was supported by the National Natural Science Foundation of China (Nos. 51974313 and 41907405) and the Natural Science Foundation of Jiangsu Province (BK20180641).

Supplementary Material Supplementary material is available in the online version of this article at https://doi.org/10.1007/s11783-021-1401-y and is accessible for authorized users.

References

Acar Y B, Alshawabkeh A N (1993). Principles of electrokinetic remediation. Environmental Science & Technology, 27(13): 2638–2647

Cappuyns V, Swennen R, Niclaes M (2007). Application of the BCR sequential extraction scheme to dredged pond sediments contaminated by Pd-Zn mining: A combined geochemical and mineralogical approach. Journal of Geochemical Exploration, 93(2): 78–90

Chen F, Li X, Ma J, Qu J, Yang Y, Zhang S (2019). Remediation of soil co-contaminated with decabromodiphenyl ether (BDE-209) and copper by enhanced electrokinetics-persulfate process. Journal of Hazardous Materials, 369: 448–455

Dong Z, Huang W, Xing D, Zhang H (2013). Remediation of soil co-contaminated with petroleum and heavy metals by the integration of electrokinetics and biostimulation. Journal of Hazardous Materials, 260: 399–408

Gomes H I, Dias-Ferreira C, Ribeiro A B (2012). Electrokinetic remediation of organochlorines in soil: Enhancement techniques and integration with other remediation technologies. Chemosphere, 87 (10): 1077–1090

Han R, Dai H, Yang C, Wei S, Xu L, Yang W, Dou X (2018). Enhanced phytoremediation of cadmium and/or benzo (a) pyrene contaminated soil by hyperaccumulator *Solanum nigrum* L. International Journal of Phytoremediation, 20(9): 862–868

Hassan I, Mohamedelhassan E, Yanful E K, Yuan Z C (2016). A review article: electrokinetic bioremediation current knowledge and new prospects. Advances in Microbiology, 06(01): 57–72

Kakosová E, Hrabák P, Černík M, Novotný V, Czinnerová M, Trögl J,

Popelka J, Kuráň P, Zoubková L, Vrtoch L (2017). Effect of various chemical oxidation agents on soil microbial communities. Chemical Engineering Journal, 314: 257–265

Li F, Guo S, Wang S, Zhao M (2020). Changes of microbial community and activity under different electric fields during electro-bioremediation of PAH-contaminated soil. Chemosphere, 254: 126880

Li H, Li X, Xiang L, Zhao H M, Li Y W, Cai Q Y, Zhu L, Mo C, Wong M H (2018). Phytoremediation of soil co-contaminated with Cd and BDE-209 using hyperaccumulator enhanced by AM fungi and surfactant. Science of the Total Environment, 613-614: 447–455

Li Y, Yin Y, Liu G, Tachiev G, Roelant D, Jiang G, Cai Y (2012). Estimation of the major source and sink of methylmercury in the Florida Everglades. Environmental Science & Technology, 46(11): 5885–5893

Lorenz P B (1969). Surface conductance and electrokinetic properties of kaolinite beds. Clays and Clay Minerals, 17(4): 223–231

Lu M, Zhang Z, Sun S, Wang Q, Zhong W (2009). Enhanced degradation of bioremediation residues in petroleum-contaminated soil using a two-liquid phase bioslurry reactor. Chemosphere, 77(2): 161–168

Lu M, Zhang Z, Wang J, Zhang M, Xu Y, Wu X (2014). Interaction of heavy metals and pyrene on their fates in soil and tall fescue (*Festuca arundinacea*). Environmental Science & Technology, 48(2): 1158–1165

Ma J, Zhang Q, Chen F, Zhu Q, Wang Y, Liu G (2020). Remediation of resins-contaminated soil by the combination of electrokinetic and bioremediation processes. Environmental Pollution, 260: 114047

Mahanta M J, Bhattacharyya K G (2011). Total concentrations, fractionation and mobility of heavy metals in soils of urban area of Guwahati, India. Environmental Monitoring and Assessment, 173(1-4): 221–240

Naghipour D, Gharibi H, Taghavi K, Jaafari J (2016). Influence of EDTA and NTA on heavy metal extraction from sandy-loam contaminated soils. Journal of Environmental Chemical Engineering, 4(3): 3512–3518

Nowack B (2002). Environmental chemistry of aminopolycarboxylate chelating agents. Environmental Science & Technology, 36(19): 4009–4016

Pletcher D, Greff R, Peat R (2010). The electrical double layer. In: Instrumental Methods in Electrochemistry. Cambridge: Woodhead Publishing lnc.

Pradas del Real A E, García-Gonzalo P, Lobo M C, Pérez-Sanz A (2014). Chromium speciation modifies root exudation in two genotypes of silene vulgaris. Environmental and Experimental Botany, 107: 1–6

Ramadan B S, Sari G L, Rosmalina R T, Effendi A J, Hadrah (2018). An overview of electrokinetic soil flushing and its effect on bioremediation of hydrocarbon contaminated soil. Journal of Environmental Management, 218: 309–321

Salzberg H W (1983). Gmelins Handbook of Inorganic Chemistry. Berlin: Spinger-Verlag

Sharma H D, Reddy K R (2004). Geoenvironmental Engineering. Hoboken: John Wiley & Sons, Inc.

Song Y, Ammami M, Benamar A, Mezazigh S, Wang H (2016). Effect of EDTA, EDDS, NTA and citric acid on electrokinetic remediation of As, Cd, Cr, Cu, Ni, Pb and Zn contaminated dredged marine sediment. Environmental Science and Pollution Research International, 23(11): 10577–10586

Suanon F, Sun Q, Dimon B, Mama D, Yu C P (2016). Heavy metal removal from sludge with organic chelators: comparative study of N, N-bis (carboxymethyl) glutamic acid and citric acid. Journal of Environmental Management, 166: 341–347

Tang W, Sun L, Shu L, Wang C (2020). Evaluating heavy metal contamination of riverine sediment cores in different land-use areas. Frontiers of Environmental Science & Engineering, 14(6): 104

Uddin M K (2017). A review on the adsorption of heavy metals by clay minerals, with special focus on the past decade. Chemical Engineering Journal, 308: 438–462

Virkutyte J, Sillanpää M, Latostenmaa P (2002). Electrokinetic soil remediation-critical overview. Science of the Total Environment, 289 (1-3): 97–121

Wang S, Guo S, Li F, Yang X, Teng F, Wang J (2016). Effect of alternating bioremediation and electrokinetics on the remediation of *n*-hexadecane-contaminated soil. Scientific Reports, 6(1): 23833

Weng C H, Yuan C (2001). Removal of Cr (III) from clay soils by electrokinetics. Environmental Geochemistry and Health, 23(3): 281–285

Yao Z, Xing J, Gu H, Wang H, Wu J, Xu J, Brookes P C (2016). Development of microbial community structure in vegetable-growing soils from open-field to plastic-greenhouse cultivation based on the PLFA analysis. Journal of Soils and Sediments, 16(8): 2041–2049

Zhang M, Guo S, Li F, Wu B (2017). Distribution of ion contents and microorganisms during the electro-bioremediation of petroleum-contaminated saline soil. Journal of Environmental Science & Health Part A, 52(12): 1141–1149